LETTERS

Wave acceleration of electrons in the Van Allen radiation belts

Richard B. Horne[1], Richard M. Thorne[2], Yuri Y. Shprits[2], Nigel P. Meredith[1], Sarah A. Glauert[1], Andy J. Smith[1], Shrikanth G. Kanekal[3], Daniel N. Baker[3], Mark J. Engebretson[4], Jennifer L. Posch[4], Maria Spasojevic[5], Umran S. Inan[5], Jolene S. Pickett[6] & Pierrette M. E. Decreau[7]

The Van Allen radiation belts[1] are two regions encircling the Earth in which energetic charged particles are trapped inside the Earth's magnetic field. Their properties vary according to solar activity[2,3] and they represent a hazard to satellites and humans in space[4,5]. An important challenge has been to explain how the charged particles within these belts are accelerated to very high energies of several million electron volts. Here we show, on the basis of the analysis of a rare event where the outer radiation belt was depleted and then re-formed closer to the Earth[6], that the long established theory of acceleration by radial diffusion is inadequate; the electrons are accelerated more effectively by electromagnetic waves at frequencies of a few kilohertz. Wave acceleration can increase the electron flux by more than three orders of magnitude over the observed timescale of one to two days, more than sufficient to explain the new radiation belt. Wave acceleration could also be important for Jupiter, Saturn and other astrophysical objects with magnetic fields.

Inward radial diffusion has long been established as the leading acceleration mechanism for outer radiation belt electrons[7,8]. According to the theory, electrons are diffused across the magnetic field by global scale fluctuations in the Earth's magnetic and electric fields at frequencies that closely match the electron drift frequencies of a few millihertz (mHz) around the Earth. The process occurs more rapidly when ultralow frequency (ULF) waves at a few millihertz are enhanced[9]. By conservation of the first adiabatic invariant (proportional to the square of the particle momentum transverse to the magnetic field divided by the magnetic field strength) the particles are accelerated if they are diffused towards the planet. However, it has recently been suggested[10,11] that electrons can be accelerated efficiently by electromagnetic waves at frequencies of a few kilohertz (kHz) propagating in the whistler mode, and known as 'whistler mode chorus'[12]. The rare and unusual events that occurred between 29 October and 4 November 2003, widely known as the Hallowe'en storms[6], provide a unique set of conditions to test the two leading acceleration theories.

Figure 1a shows the electron particle flux at energies 2–6 MeV during the Hallowe'en storms. The data are presented as a function of L (where L is the distance from the centre of the Earth to the point where a magnetic field line crosses the equator, measured in Earth radii). Before the storms, the outer radiation belt is centred near $L = 3.5$. As the first storm begins on 29 October, there is a large depletion in the electron flux for $L > 3.0$, and a re-formation of the outer radiation belt near $L = 2.5$. The intensity of the new belt varies, but increases significantly from 1 November for a period of three or four days. The flux subsequently decays and the outer
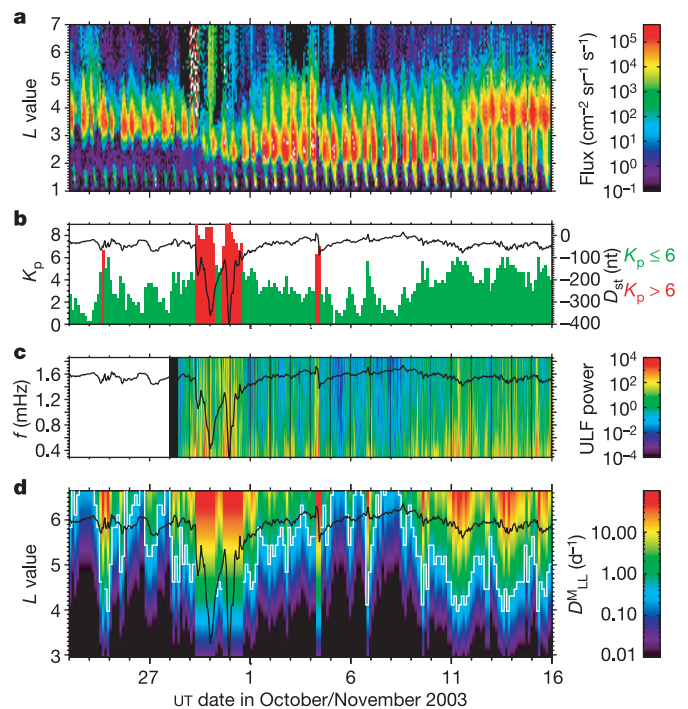

Figure 1 | Satellite and ground based data during the Hallowe'en storm. **a**, Flux of 2–6 MeV electrons measured by the Solar Anomalous and Magnetospheric Particle Explorer (SAMPEX) satellite, colour coded according to the colour bar on the right. The data are averaged over each orbit. SAMPEX is a polar orbiting satellite; the flux modulations are due to the satellite passing over the South Atlantic Anomaly region where the outer radiation belt penetrates closer to the Earth. **b**, the K_p index (colour coded) and the D_{st} index (solid line). The former is a measure of the global disturbance in the Earth's magnetic field and is related to ULF waves, and the latter is a measure of electrical current systems and exhibits rapid negative excursions when geomagnetic storms are triggered. The Hallowe'en storms started on 29 October and ended by 4 November. The D_{st} index is also included in **c** and **d**. **c**, ULF wave power measured on the ground by Automatic Geophysical Observatory A80 in Antarctica at $L = 6.2$. The data are differenced to help identify signals and colour coded in nT^2 Hz. **d**, Radial diffusion coefficient D_{LL}^M for magnetic field fluctuations, valid for $K_p < 6$. When $K_p > 6$, they are calculated for $K_p = 6$. The solid white line shows the L shell for which the radial diffusion coefficient is $0.5\,d^{-1}$.

[1]British Antarctic Survey, Madingley Road, Cambridge CB3 0ET, UK. [2]Department of Atmospheric and Oceanic Sciences, University of California Los Angeles, 405 Hilgard Avenue, Los Angeles, California 90095-1565, USA. [3]Laboratory for Atmospheric and Space Physics, University of Colorado, 1234 Innovation Drive, Boulder, Colorado 80303-7814, USA. [4]Department of Physics, Augsburg College, Minneapolis, Minnesota 55454, USA. [5]STAR Laboratory, Stanford University, Stanford, California 94305, USA. [6]Department of Physics and Astronomy, University of Iowa, Iowa City, Iowa 52242-1479, USA. [7]LPCE, 3A Avenue de la recherche scientifique, 45071 Orleans, Cedex 2, France.
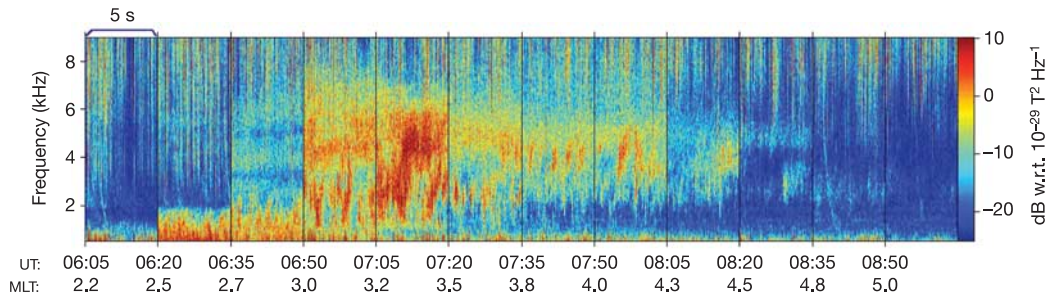
Figure 2 | Waves observed at Palmer station, Antarctica, on 1 November 2003. The power spectral density of electromagnetic waves (in the whistler mode) is shown in dB with respect to 10^{-29} T^2 Hz^{-1}. Each panel is a five-second snapshot starting at the universal time (UT) indicated, with approximate magnetic local time (MLT) also shown. Wave power (identified as whistler mode chorus) is significantly enhanced between 2 kHz and 6 kHz on 1 November 2003 between 06:50 UT and 08:35 UT when the station was in daylight, which causes strong attenuation of the waves as they pass through the upper atmosphere. Sunrise at Palmer at 100 km altitude is 05:00 UT on this day. The emissions fade owing to increased absorption as the Sun rises further, and possibly owing to drift of the source of low energy electrons out of the station viewing area. Strong waves were also detected at Halley Research station at $L = 4.3$ during the storms (not shown).

radiation belt is re-formed after 10 November at its usual location near $L = 4$.

A key feature of this event is that after 1 November the electron flux increases as the global level of magnetic activity, as measured by the K_p index (Fig. 1b), decreases and as conditions recover from the magnetic storms, as indicated by the D_{st} index returning to near zero (Fig. 1b). Data from one of the Automatic Geophysical Observatories, operated by the British Antarctic Survey in Antarctica, also show that the power level of ULF waves decreased as the flux increased (Fig. 1c). As ULF waves drive particle transport across the magnetic field, the data suggest that radial diffusion may not be the most effective process responsible for the flux increase.

The K_p index is often used as a proxy to determine the efficiency of inward radial diffusion[13]. Using this proxy, we have calculated the radial diffusion coefficient, D_{LL}, which determines the timescale for inward electron transport. The proxy is only valid for $K_p < 6$, and thus the results are not valid during 29, 30 and 31 October when the new belt began to form. Thus it is possible that inward radial diffusion could contribute to the formation of the new belt[14] before 1 November. However, from 1 November onwards, the flux in the new belt increased by a factor of ~10, but D_{LL} decreased, and was comparable to the values before the new belt (on 28 October) when there was no flux increase (compare white lines). In fact D_{LL} was even larger on 11 and 13 November when the new belt was decaying. Thus
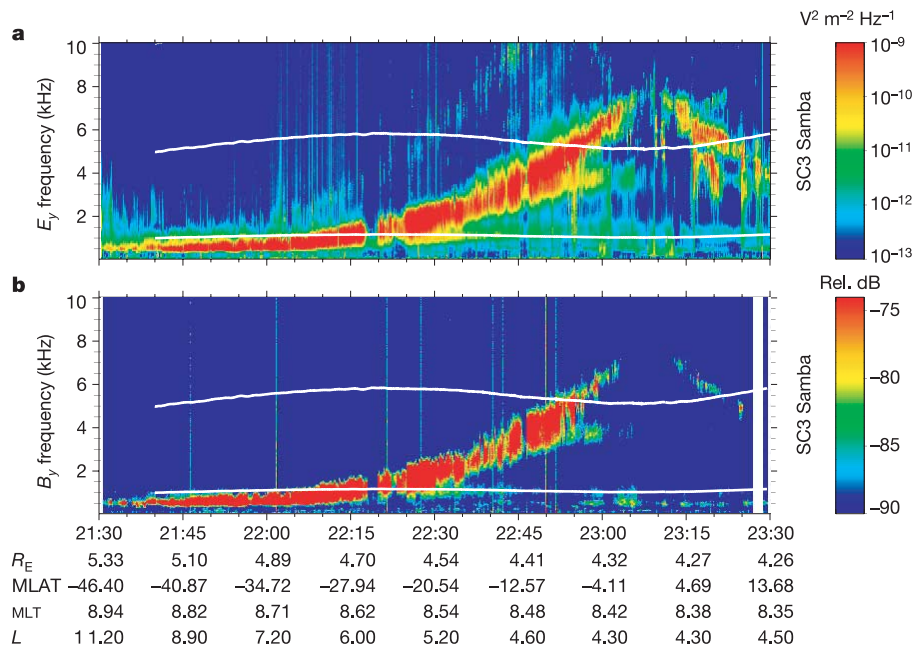

Figure 3 | Waves observed by the Cluster spacecraft. Data from the Wideband (WBD) plasma wave instrument on one of the four Cluster spacecraft (Samba) is shown for 31 October 2003. The wave electric field E_y transverse to the ambient magnetic field is shown in **a**, and wave magnetic field B_y in **b**. The colour bars on the right give the calibrated wave power spectral density for the wave electric field (**a**), and relative wave power spectral density (in dB) for the wave magnetic field (**b**). The instrument cycles between the electric and magnetic antennas recording data for 42 s (electric) and 10 s (magnetic). The data obtained from the electric (magnetic) antenna during each cycle is dilated to fill the data gap that is created when WBD is obtaining data from the magnetic (electric) antenna. Both antennas detect chorus waves indicating that the waves are electromagnetic. Magnetic wave power (**b**) above 4 kHz is attenuated owing to low pass filtering in the search coils and is thus not representative of the true wave power. The white lines denote $0.5f_{ce}$ and $0.1f_{ce}$, where f_{ce} is the local electron cyclotron frequency ($f_{ce} = |e|B/(2\pi m_e)$ where $|e|$ is the electron charge, m_e is the electron mass and B is the ambient magnetic field obtained from the fluxgate magnetometer on board the spacecraft. At the magnetic equator f_{ce} is approximately 10 kHz, and the electron plasma frequency f_{pe}, obtained from the Whisper sounder, is approximately 35 kHz. At 22:46 UT the peak wave power spectral density is ~6×10^{-6} nT^2 Hz^{-1} at ~$0.35f_{ce}$, and tends to increase with magnetic latitude (MLAT).

inward radial diffusion alone cannot explain the increase in 2–6 MeV electron flux from 1 November onwards.

Electron acceleration by whistler mode chorus waves is the alternative leading theory[10,11]. The waves are excited by an unstable anisotropic[15] distribution of ~10 keV electrons, possibly via non-linear interactions[16], and transfer the energy to accelerate a fraction of the electrons to very high energies. Acceleration occurs via a cyclotron resonance where the wave frequency is Doppler shifted to the cyclotron frequency of the particles. For a broad band of waves, typically observed inside the Earth's magnetic field, resonance can extend from energies of ~10 keV up to several MeV (ref. 11). Such local acceleration is most effective in regions where the ratio of the electron plasma to cyclotron frequency (f_{pe}/f_{ce}) is low[17], typically <4. Under normal conditions, the plasma density is high and f_{pe}/f_{ce} is large near $L = 2.5$, and hence wave acceleration is not expected. However, during the Hallowe'en storms the region of high density was confined to $L < 2.0$ on 31 October, and remained inside $L = 2.5$ between 06–12 magnetic local time (MLT) until about 4 November[6]. Using a dipole magnetic field, and a density model appropriate to this region[18], we find $f_{pe}/f_{ce} \approx 2.5$, which suggests wave acceleration could be important.

Unfortunately, there are no direct wave observations in the new radiation belt near $L = 2.5$ during this event. However, whistler mode chorus waves can be guided along the magnetic field, and were detected at Palmer station, Antarctica, at $L = 2.4$ on 1 November (Fig. 2). Chorus waves are only observed at Palmer during very large
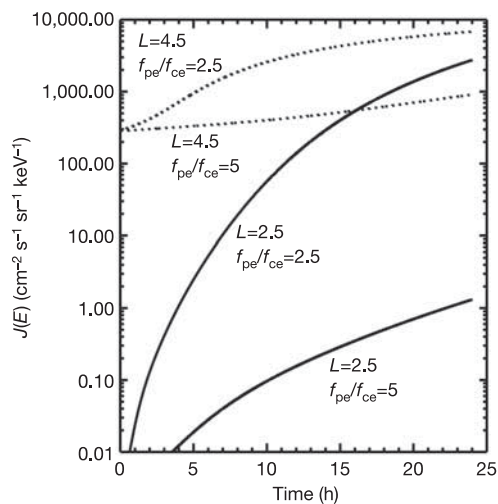
storms and so the observation, particularly during sunlight, is exceptional. Similar waves were observed on 29, 30 and 31 October 2003. Since chorus waves are generated in space, in low-density regions[19], the ground observations provide strong evidence for waves in space near the equator.

Strong whistler mode chorus waves were also detected at larger L ($L > 4.3$) on 31 October by the Cluster satellites (Fig. 3). The active sounder experiment on the satellite also provided an accurate measurement of $f_{pe}/f_{ce} = 3.5$ at the equator, and found that f_{pe}/f_{ce} decreased with increasing latitude, providing the right conditions for wave acceleration.

Using a one-dimensional Fokker-Planck equation[20], we have calculated the increase in electron flux due to whistler mode chorus waves (Fig. 4). Loss and acceleration due to chorus waves are included via diffusion rates calculated from the PADIE code[21] (see Supplementary Data). Since chorus waves are usually present outside the high-density region during magnetic storms[19], we assume that the wave power spectral density observed by Cluster at $L = 4.3$ are also typical of $L = 2.5$. We also assume that the waves only exist for 6 h out of 24 h of MLT, as shown by the statistical distribution of wave occurrence[19].

At $L = 2.5$, for $f_{pe}/f_{ce} = 2.5$, the electron flux increases from the noise level and exceeds the average flux in the heart of the outer radiation belt ($L = 4.5$) within 24 h. This is more than sufficient to account for the enhancement in the new radiation belt after 1 November. For comparison, at $L = 4.5$ the flux increases by a factor of ~20 for $f_{pe}/f_{ce} = 2.5$. To illustrate the sensitivity of the results, the flux increase is also shown for $f_{pe}/f_{ce} = 5$. Although the flux increases at $L = 2.5$ by a factor of ~100 within 24 h, it remains below detectable levels. Thus wave acceleration is most effective owing to the low density at $L = 2.5$ as a result of the confinement of the high-density region to $L < 2.5$ during this event[9]. Losses are not significant, since low values of f_{pe}/f_{ce} increase the phase velocity of the waves so that energy diffusion is more effective than pitch angle diffusion, particularly for energies >300 keV.

After 1 November the flux in the new radiation belt increased from a level that had already been enhanced. To represent a higher initial level, we repeated the calculation for a minimum flux level of $1 \, cm^{-2} \, s^{-1} \, sr^{-1} \, keV^{-1}$, and then $10^2 \, cm^{-2} \, s^{-1} \, sr^{-1} \, keV^{-1}$. After 24 h, the flux at $L = 2.5$, $f_{pe}/f_{ce} = 2.5$, reached approximately the same level as shown in Fig. 4.

The results suggest that wave–particle interactions not only play an important role determining the structure of the radiation belts via losses to the atmosphere[22], but also are a principal mechanism for their formation in low-density regions. The theory is applicable to particle acceleration at Jupiter and Saturn, and to other astrophysical objects with magnetic fields.

Figure 4 | Simulation results. Electron flux at 1 MeV due to wave acceleration for $L = 2.5$ (solid lines) and $L = 4.5$ (dotted lines). The flux was obtained by solving a one-dimensional Fokker-Planck equation given by equation (9) in ref. 20, and includes losses due to pitch angle diffusion. It is assumed that the electron pitch angle distribution is isotropic. The diffusion rates (bounced-averaged pitch angle and energy) corresponding to a peak power spectral density of $\sim 2 \times 10^{-6} \, nT^2 \, Hz^{-1}$ are given in Supplementary Table 1. The diffusion rates were scaled down by a factor of 4 (to represent the fraction of MLT over which the waves are present), and interpolated onto a high-resolution grid. The loss timescale was assumed to be equal to the inverse of the pitch angle diffusion rate at the edge of the loss cone. Acceleration rates exceed loss rates for $E > 300$ keV (ref. 20). Since SAMPEX did not measure electrons below 2 MeV, the initial flux was obtained by averaging CRRES satellite data for low magnetic activity (using auroral electrojet index, AE < 100 nT) at $2.4 < L < 2.6$ and $4.4 < L < 4.6$ for energies between 153 keV and 1.58 MeV. At $L = 2.5$ the flux for $E > 1.09$ MeV was at the noise level ($10^{-2} \, cm^{-2} \, s^{-1} \, sr^{-1} \, keV^{-1}$) and set to zero in the model. The flux was interpolated onto a high-resolution grid, and converted into phase space density. Fixed boundary conditions were used with the flux set to the initial value at 153 keV, and zero at 11 MeV. The code calculates phase space density, and converts the results back into flux for comparison with data.

1. Van Allen, J. A. in *Discovery of the Magnetosphere* (eds Gillmor, C. S. & Spreiter, J. R.) 235–251 (Vol. 7, History of Geophysics, American Geophysical Union, Washington DC, 1997).
2. Baker, D. N., Blake, J. B., Klebesadel, R. W. & Higbie, P. R. Highly relativistic electrons in the Earth's outer magnetosphere 1. Lifetimes and temporal history 1979–1984. *J. Geophys. Res.* **91**, 4265–4276 (1986).
3. Li, X., Baker, D. N., Kanekal, S. G., Looper, M. & Temerin, M. Long term measurements of radiation belts by SAMPEX and their variations. *Geophys. Res. Lett.* **28**, 3827–3830 (2001).
4. Baker, D. N., Allen, J. H., Kanekal, S. G. & Reeves, G. D. Disturbed space environment may have been related to pager satellite failure. *Eos* **79**, 477 (1998).
5. Webb, D. F. & Allen, J. H. Spacecraft and ground anomalies related to the October-November 2003 solar activity. *Space Weath.* **2**, doi:10.1029/2004SW000075 (2004).
6. Baker, D. N. *et al.* An extreme distortion of the Van Allen belt arising from the Hallowe'en solar storm in 2003. *Nature* **432**, 878–881 (2004).
7. Falthammar, C.-G. Effects of time dependent electric fields on geomagnetically trapped radiation. *J. Geophys. Res.* **70**, 2503–2516 (1965).
8. Schulz, M. & Lanzerotti, L. J. *Particle Diffusion in the Radiation Belts* (Springer, New York, 1974).

9. Elkington, S. R., Hudson, M. K. & Chan, A. A. Acceleration of relativistic electrons via drift resonant interactions with toroidal-mode Pc-5 ULF oscillations. *Geophys. Res. Lett.* **26**, 3273–3276 (1999).

10. Summers, D., Thorne, R. M. & Xiao, F. Relativistic theory of wave-particle resonant diffusion with application to electron acceleration in the magnetosphere. *J. Geophys. Res.* **103**, 20487–20500 (1998).

11. Horne, R. B. & Thorne, R. M. Potential waves for relativistic electron scattering and stochastic acceleration during magnetic storms. *Geophys. Res. Lett.* **25**, 3011–3014 (1998).

12. Tsurutani, B. T. & Smith, E. J. Postmidnight chorus: A substorm phenomenon. *J. Geophys. Res.* **79**, 118–127 (1974).

13. Brautigam, D. H. & Albert, J. M. Radial diffusion analysis of outer radiation belt electrons during the October 9, 1990, magnetic storm. *J. Geophys. Res.* **105**, 291–309 (2000).

14. Shprits, Y. Y. & Thorne, R. M. Time dependent radial diffusion modeling of relativistic electrons with realistic loss rates. *Geophys. Res. Lett.* **31**, doi:10.1029/2004GL019591 (2004).

15. Kennel, C. F. & Petschek, H. E. Limit on stably trapped particle fluxes. *J. Geophys. Res.* **71**, 1–28 (1966).

16. Helliwell, R. A. A theory of discreet emissions from the magnetosphere. *J. Geophys. Res.* **72**, 4773–4790 (1967).

17. Horne, R. B., Glauert, S. A. & Thorne, R. M. Resonant diffusion of radiation belt electrons by whistler-mode chorus. *Geophys. Res. Lett.* **30**, doi:10.1029/2003GL016963 (2003).

18. Sheeley, B. W., Moldwin, M. B., Rassoul, H. K. & Anderson, R. R. An empirical plasmasphere and trough density model: CRRES observations. *J. Geophys. Res.* **106**, 25631–25641 (2001).

19. Meredith, N. P., Horne, R. B., Thorne, R. M. & Anderson, R. R. Favoured regions for chorus-driven electron acceleration to relativistic energies in the Earth's outer radiation belt. *Geophys. Res. Lett.* **30**, 1871, doi:10.1029/2003GL017698 (2003).

20. Horne, R. B. *et al.* Timescale for radiation belt electron acceleration by whistler mode chorus waves. *J. Geophys. Res.* **110**, A03225, doi:10.1029/2004JA010811 (2005).

21. Glauert, S. A. & Horne, R. B. Calculation of pitch angle and energy diffusion coefficients with the PADIE code. *J. Geophys. Res.* **110**, A04206, doi:10.1029/2004JA010851 (2005).

22. Lyons, L. R. & Thorne, R. M. Equilibrium structure of radiation belt electrons. *J. Geophys. Res.* **78**, 2142–2149 (1973).